CrystEngComm

Accepted Manuscript

ROYAL SOCIETY OF CHEMISTRY

www.rsc.org/crystengcomm

Cite this: DOI: 10.1039/c0xx00000x

www.rsc.org/xxxxxx

ARTICLE TYPE

Diversity of felodipine solvates: structure and physicochemical properties

Artem O. Surov,[a] Katarzyna A. Solanko,[b] Andrew D. Bond,[b§] Annette Bauer-Brandl,[b] German L. Perlovich[a]

Received (in XXX, XXX) Xth XXXXXXXXX 20XX, Accepted Xth XXXXXXXXX 20XX
DOI: 10.1039/b000000x

Solvates of the calcium-channel blocking agent felodipine with three structurally related common organic solvents, acetone (**ATN**), dimethyl sulfoxide (**DMSO**) and acetophenone (**APN**), are described. A relationship between the felodipine packing arrangement in all known solvates and the van der Waals volume of the solvent molecule is established. Intermolecular interaction energies in the crystals are examined using the PIXEL approach in order to rationalize the difference between alternative molecule packing arrangements. DSC studies show that the desolvation onset temperatures of the solvates are closely comparable, despite the large difference in the boiling points of the solvent molecules. The enthalpies of formation derived from the calorimetric data for the solvates are also found to be similar, despite the difference in the van der Waals volume of the solvent molecules.

Introduction

In many cases, active pharmaceutical ingredients (APIs) are established to exist in different crystal forms such as polymorphs or solvates/hydrates.[1] The latter in general play a significant part in drug development, and solid-form screening to identify solvates/hydrates is a crucial prerequisite for consistent manufacturing and processing of drugs.[2] Accidental solvate formation is highly undesirable during processing of drugs due to lack of predictability and, as a consequence, potentially uncontrollable changes of the physicochemical properties of a product. On the other hand, solvates of APIs with pharmaceutically relevant solvents can improve some physicochemical properties of drugs, such as solubility and dissolution rate.[3] Moreover, desolvation of solvates can be a method to discover and prepare new polymorphic forms that may be inaccessible *via* ordinary crystallization techniques.[4]

In this paper, we focus on studying the structures and physicochemical properties of solvates of the API felodipine with three structurally related common organic solvents, acetone (**ATN**), dimethyl sulfoxide (**DMSO**) and acetophenone (**APN**). Felodipine [systematic name: ethyl methyl 4-(2,3-dichlorophenyl)-1,4-dihydro-2,6-dimethyl-3,5-pyridinedicarboxylate] belongs to a family of dihydropyridine calcium channel blockers that are used for treatment of hypertension and regulation of arterial pressure (Fig. 1).[5]

Four polymorphic forms of felodipine have been identified to date: forms I and II have been known for a long time,[6] and we have quite recently reported forms III and IV.[7] Polymorphism of felodipine co-crystals with 4,4′-bipyridine in 1:1 and 2:1 molar ratios has been studied,[8] and a hydrated co-crystal of felodipine with diazabicyclo[2.2.2]octane (DABCO) has also been reported.[9] In addition, felodipine exhibits a strong propensity for solvate formation with various solvents. The solvate of felodipine with acetone was described and characterized for the first time by Rollinger and Burger[10] using DSC, IR spectroscopic and powder X-ray diffraction techniques. However, a single-crystal X-ray structure of the solvate has not previously been reported. The crystal structure of a felodipine solvate with formamide ([**Fel+FA**]) has been published by Lou *et al.*,[11] and two solvates with dimethylformamide (**DMF**) and *N*-methylformamide (**N-MeFA**) have been studied by Perlovich *et al.*[12]

We have also reported felodipine solvates with the structurally-related high-boiling point solvents, dimethylacetamide (**DMAA**), dimethylethyleneurea (**DMEU**) and tetramethylurea (**TMU**).[13] In this work, we consider all experimental data obtained so far in a systematic manner, with an aim to rationalize the relationships between the crystal structures of the solvates and their observed physicochemical properties, which is an important issue in a pharmaceutical solid-form development.

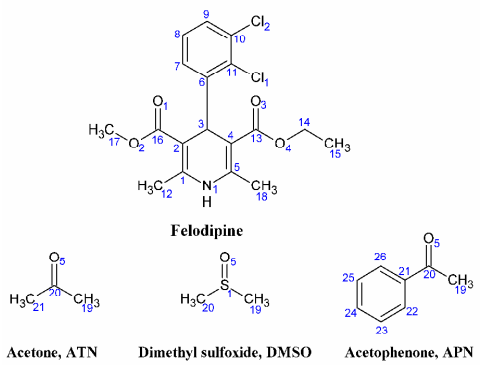

Fig.1 Structure of felodipine and investigated solvent molecules with atom numbering.

Material and Methods

Compounds and solvents

Felodipine ($C_{18}H_{19}Cl_2NO_4$, MW 384.26, 99.5%, racemate) was produced by Xiamen (Fine Chemical Import @ Export Co., LTD) and received as polymorphic form I. All solvents were purchased from Sigma-Aldrich (Denmark). All of the starting materials were used without further purification.

Crystallization procedure

The solvates of felodipine with dimethyl sulfoxide and acetophenone were prepared by dissolving felodipine in each respective solvent preheated to 60°C. The obtained clear solution was slowly cooled and then allowed to evaporate under ambient conditions. Single crystals of the felodipine solvate with acetone were obtained by slow evaporation of a saturated felodipine solution stored at -20°C in a freezer. Crystals obtained from the crystallization batches were air dried before being subjected to further analysis.

X-ray diffraction

Single-crystal X-ray diffraction data for [**Fel+ATN**] and [**Fel+APN**] were collected on a Bruker-Nonius X8-APEXII CCD diffractometer using MoKα radiation (λ = 0.7107 Å) at 150(1) K. Data for [**Fel+DMSO**] were collected under ambient conditions using a Bruker P4 diffractomer with MoKα radiation (λ = 0.7107 Å). The structures were solved by direct methods and refined by full matrix least-squares on F^2 with anisotropic thermal parameters for all non-hydrogen atoms.

Aqueous dissolution measurements

Dissolution measurements were carried out by the shake-flask method at 25.0 ± 0.1°C. Samples were suspended in 10 ml of water in glass tubes. The amount of felodipine solvate dissolved was measured by taking aliquots of 2 ml of the respective media and measuring concentration in a UV-vis spectrophotometer (Cary 50, Varian Inc.). The solid phase was removed by isothermal filtration (VWR syringe filter, PTFE, 0.45 μm). The results are stated as the average of at least three replicated experiments.

Solution calorimetry

Enthalpies of solution were measured by using an ampoule-type isoperibolic calorimeter with a titanium reaction vessel volume of 50 cm^3.[14] The automated control scheme allowed the temperature to be maintained with an accuracy greater than 6×10^{-4} K. The temperature and thermal sensitivities of the calorimeter measuring cell were 10^{-4} K and 10^{-3} J, respectively. The instrumental errors were 0.6–1%. The accuracy of weight measurements corresponded to ±0.01 mg. Due to small values of the solution heat effects, a correction ($q(T)$) was introduced to account for the heat of breaking of the ampoule and evaporation of the solvent in the ampoule free volume: q(293.15 K) = 0.034 J, q(303.15 K) = –0.018 J, q(318.15 K) = –0.059 J. Other corrections were negligibly small. The calorimeter was calibrated using KCl (Merck analysis grade >99.5%) in water over a wide concentration interval with more than 20 measurements made. The obtained standard value of solution enthalpy was 17240 ± 36 $J \cdot mol^{-1}$, which is in good agreement with the value 17241 ± 18 $J \cdot mol^{-1}$ recommended by IUPAC.[15] A minimum of four measurements were performed for each of the analyzed samples.

Differential scanning calorimetry (DSC)

Thermal analysis was carried out on a DSC 204 F1 Phoenix differential scanning heat flux calorimeter (NETZSCH, Germany) with a high sensitivity μ-sensor. The sample was heated at a rate of $10°C \cdot min^{-1}$ in an Ar atmosphere over the temperature range of 25 to 170-180°C and cooled with gaseous N_2. The temperature calibration was performed against six high-purity substances: cyclohexane (99.96%), Hg (99.99+%), biphenyl (99.5%), In (99.999%), Sn (99.999%), and Bi (99.9995%). The accuracy of the weighing procedure was ±0.01 mg.

Thermogravimetric analysis (TGA)

TGA was performed on a TG 209 F1 Iris thermomicrobalance (Netzsch, Germany). Approximately 10 mg of the sample was added to a platinum crucible. The samples were heated over the temperature range of 25 to 250°C at a constant heating rate of $10°C \cdot min^{-1}$. The samples were purged with a stream of flowing dry Ar throughout the experiment at 30 $mL \cdot min^{-1}$.

Hot stage microscopy (HSM)

Thermomicroscopic investigations were performed with an optical polarizing microscope (Altami Polar 312) equipped with a hot stage and Microstat 100 temperature controller. The microscope images were recorded with an Altami CMOS digital camera using *Altami Studio* image capture software. The samples were heated over a temperature range of 25–170°C at a constant heating rate of $2°C \cdot min^{-1}$. The hot stage was calibrated using USP melting point standards (vanillin, acetanilide, phenacetin, caffeine).

Computational procedures

The van der Waals molecular volume (V_{vdw}) in the crystal lattice was calculated using the spatial descriptors in *Materials Studio*. Intermolecular interaction energies were analyzed using the PIXEL approach developed by Gavezzotti.[16] This method provides quantitative determination of crystal lattice energies and pairwise intermolecular interactions, with a breakdown of these energies into coulombic, polarization, dispersion and repulsion terms.

Results and Discussion

Crystal structures

Crystallographic data are summarized in Table 1, and the molecular units of the solvates are shown in Fig. 2. In each structure, the solvent molecule accepts an N–H···O hydrogen bond from the felodipine molecule. In the [**Fel+DMSO**] solvate, the S atom of the solvent molecule is disordered over two positions, with the major component having a site-occupancy factor of 0.857(6) (Fig.2a). The O atom (involved in the hydrogen bond) and the C atoms of the methyl group occupy consistent positions. This type of disorder is common in DMSO solvates. According to Cruz-Cabeza *et al*., almost 50% of DMSO solvate structures found in the Cambridge Structural Database show structural disorder.[17] The ester groups of felodipine also show some disorder, corresponding to exchange of the positions of the

OMe and OEt groups.

Table 1 Crystallographic data for **[Fel+DMSO]**, **[Fel+APN]** and **[Fel+ATN]**

Compound reference	**[Fel+DMSO]**	**[Fel+APN]**	**[Fel+ATN]**
Chemical formula	$C_{18}H_{19}Cl_2NO_4$•C_2H_6OS	$C_{18}H_{19}Cl_2NO_4$•C_8H_8O	$C_{18}H_{19}Cl_2NO_4$•C_3H_6O
Formula Mass	462.37	504.39	442.33
Crystal system	triclinic	orthorhombic	monoclinic
a/Å	8.660(3)	7.3940(7)	9.1774(8)
b/Å	9.816(3)	11.4991(10)	16.6983(15)
c/Å	13.782(4)	29.003(2)	14.3375(11)
α/°	87.37(2)	90	90
β/°	79.17(3)	90	105.865(4)
γ/°	77.79(3)	90	90
Unit cell volume/Å^3	1124.6(6)	2466.0(4)	2113.5(3)
Temperature/K	293(2)	150(2)	150(2)
Space group	*P*–1	$P2_12_12_1$	$P2_1/n$
No. of formula units per unit cell, *Z*	2	4	4
Calculated density, *ρ*/g cm^{-3}	1.365	1.359	1.390
Absorption coefficient, *μ*/mm^{-1}	0.412	0.301	0.340
No. of reflections measured	4671	11352	33416
No. of independent reflections	3924	4368	4003
R_{int}	0.042	0.036	0.046
*R*1 ($I > 2\sigma(I)$)	0.084	0.053	0.040
*wR*2 (all data)	0.242	0.119	0.086
Goodness of fit on F^2	1.04	1.07	1.04
CCDC No.	1048182	1048181	1048180

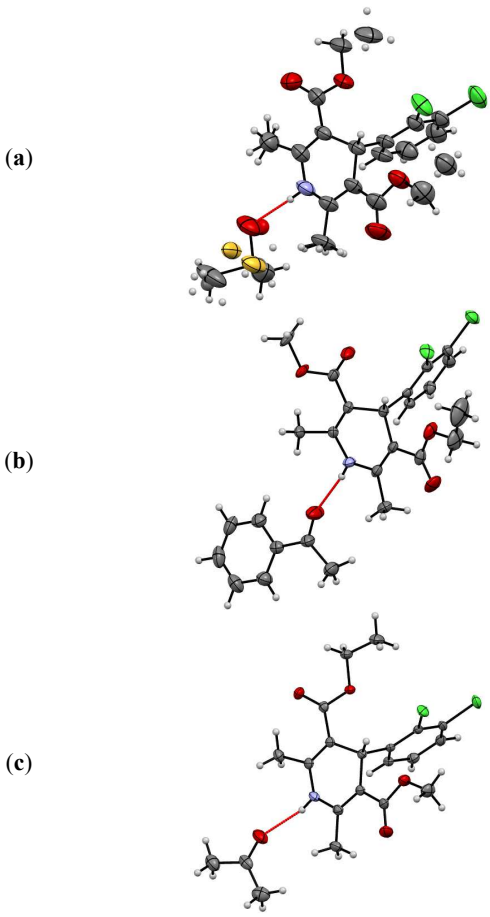

Fig.2 Molecular units in (**a**) [**Fel**+**DMSO**] form I; (**b**) **[Fel+APN]**; (**c**) [**Fel+ATN**]. Displacement ellipsoids are shown at 50% probability.

The same type of disorder is observed in the previously published [**Fel+DMAA**] and [**Fel+DMEU**] structures.

The solvent molecule of **[Fel+APN]** is fully ordered and the plane of the **APN** molecule forms an angle of *ca* 12° with the 1,4-dihydropyridine ring (Fig.2b). For the [**Fel+ATN**] solvate, the 1,4-dihydropyridine ring of **Fel** and the plane of the hydrogen-bonded **ATN** molecule form an angle of *ca* 9.4° (Fig. 2c).

In our previous works, attention has been paid to the molecular conformation of felodipine in the known polymorphs, co-crystals and solvates.[7,8,13] The molecular conformation of felodipine is essentially identical in [**Fel**+**ATN**] and [**Fel**+**DMSO**], and it corresponds to a relatively low-energy molecular conformer, which is observed in the most of the known felodipine solvates. In [**Fel**+**APN**], the OMe ester group adopts an opposite orientation, so that the C=O group points away from the Me group of the 1,4-dihydropyridine ring. This conformation is found to be similar to that in **[Fel+TMU]** and **[Fel+FA]** (see details in the Supporting Information).

In the [**Fel**+**DMSO**] solvate, the **Fel** molecules are packed in a centrosymmetric "back-to-back" manner, which is one of the main structural features in the polymorphs of pure felodipine (see Figs. S2-S4 in the Supporting Information).[7] The interplanar distance of 3.90 Å for these "back-to-back" contacts at the longer end of those observed in felodipine polymorphs I–IV (3.65–3.87 Å). The packing arrangement of the [**Fel**+**DMSO**] solvate can be described as parallel layers of felodipine molecules (in the (01–1) planes), where the space between layers is occupied by **DMSO** (Fig 3a).

In the **[Fel+APN]** solvate, the molecules are arranged as alternating bilayers of **Fel** and single layers of **APN** molecules parallel to the (001) planes. Thus, there are clear regions with the solvent-solvent interactions and regions where only felodipine molecules interact. At the inside of each **Fel** bilayer, the molecules are packed in a "side-on" manner so that the dichlorobenzene rings approach the backside of the neighbouring 1,4-dihydropyridine rings. A similar packing arrangement is observed in the **[Fel+TMU]** solvate. In addition, C24-H24…O3

interactions are formed between the phenyl ring of **APN** and the OMe group of **Fel** (Fig 3b).

In the case of the **[Fel+ATN]** solvate, the structure does not show any clear separation of the **Fel** and solvent molecules, as observed for the **[Fel+APN]**. The hydrogen-bonded **ATN** molecules are situated between the neighboring **Fel** molecules forming a "face-to-face" contact with the dichlorobenzene rings (Fig 3c). The crystal structure of this solvate is also based on "back-to-back" interaction between **Fel** molecules, as observed for the [**Fel+DMSO**] solvate. However, every second centrosymmetric "back-to-back" molecular pair in **[Fel+APN]** is turned 90° to each other to form a ladder-type structure (Fig 3d). The perpendicular orientation of the neighbouring felodipine molecules leads to formation of C8-H8…O1 and C9-H9…O3 interactions between dichlorobenzene rings and OMe/OEt groups. This type of packing arrangement is not observed in any of the other known felodipine polymorphs, solvates or co-crystals.

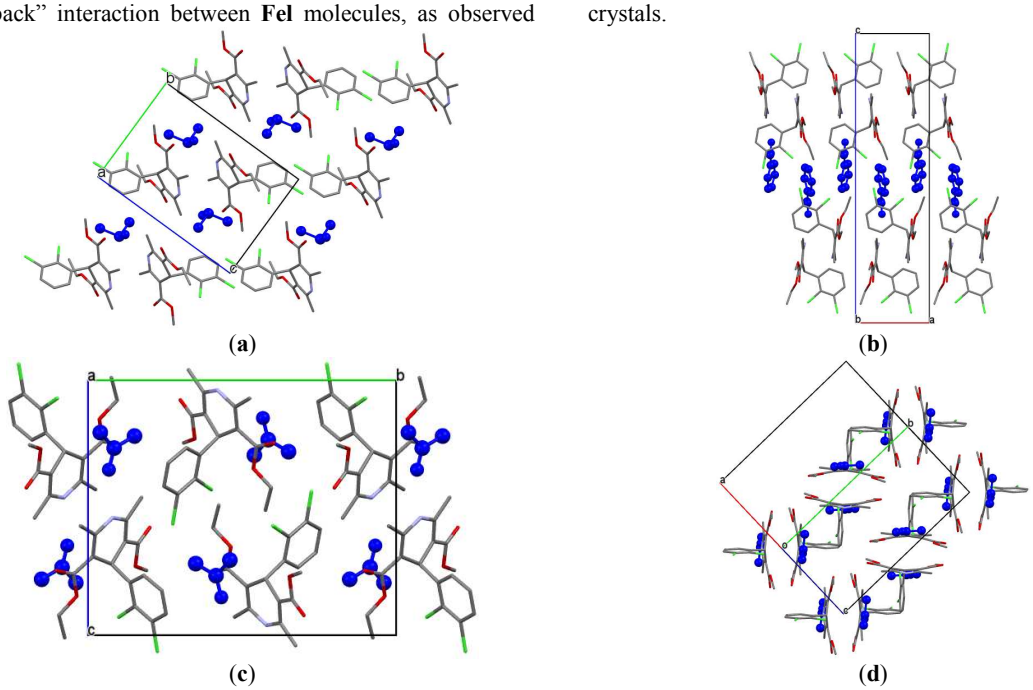

Fig.3 Molecular packing projections for (**a**) [**Fel+DMSO**]; (**b**) **[Fel+APN]**; (**c**), (**d**) **[Fel+ATN]** solvates. Solvent molecules are coloured in blue. H atoms are omitted.

As mentioned in the Introduction, six solvates of felodipine are already reported in the literature. The crystal structures of the solvates (including the three new ones reported here) can be divided into two groups: those based on "back-to-back" packing arrangements of the **Fel** molecules and those where the units are packed in a "side-on" manner. Apparently, the **Fel-Fel** molecule arrangement should depend on the interaction energy between solvent and Fel as well as the spatial characteristics the solvent molecule that is present in the solvate structure. Different characteristics of the solvent molecules such as the ability to form donor-acceptor interactions and the topological similarity were tested in order to find a relationship between properties of the solvent and the crystal packing arrangement of the felodipine molecules (see details in the Supporting Information). The results, however, were not able to provide a clear answer to the question of interest. The most suitable parameter to consider is found to be the van der Waals volume (V_{vdw}) of the solvent molecule. Since all the solvent molecules have only one site of hydrogen bonding, this parameter is responsible for the most of the weak van der Waals interactions that occur between molecules in a crystal.

Scheme 1 illustrates the change in the crystal packing arrangement as the van der Waals volume (V_{vdw}) of the solvent molecule increases.

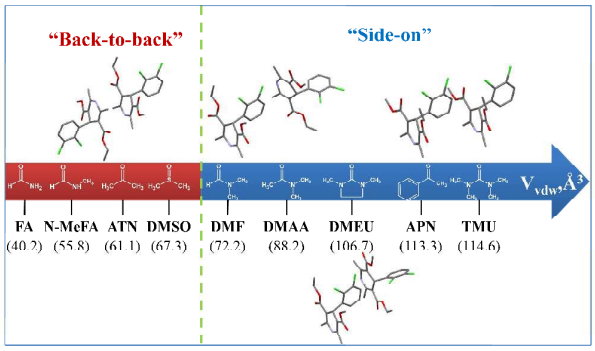

Scheme 1 The change in the crystal packing arrangement of the solvates with increasing van der Waals volume (V_{vdw}) of the solvent molecule

It is evident that at relatively small V_{vdw} (40 Å^3 < V_{vdw} < 70 Å^3) the **Fel** molecules tend to form a "back-to-back" packing arrangement, which is also one of the main structural features in the crystals of the non-solvated compound. Formation of a "side-on" organization is observed when the van der Waals volume of the solvent molecule is greater than 70Å^3. In [**Fel+DMF**] and [**Fel+DMAA**], the neighboring **Fel** molecules are turned so that their dichlorobenzene rings lie approximately perpendicular to each other, while in [**Fel+DMEU**], the dichlorobenzene planes form an angle of *ca* 64°. Further increase of V_{vdw} of the solvent molecule over 110 Å^3 also leads to modification of the packing

arrangement within the framework of a "side-on" crystal organization. In [**Fel+APN**] and [**Fel+TMU**], the **Fel** molecules are arranged into double layers of centrosymmetric units. Inside of each layer the molecules are related by crystallographic translation (along *a*).

Thus, "side-on" and "back-to-back" structure organizations are two alternative packing arrangements for the **Fel** molecules in the solvates. It seems that the "side-on" interactions are less stable, since they are not seen in any of the polymorphs of pure felodipine. The stabilization of such structures is expected to be on account of differing intermolecular interactions with solvent molecules.

In order to verify this assumption, the intermolecular interaction energies in the crystal structures were calculated using the PIXEL approach of Gavezzotti[16] (Table 2). It is evident that dispersion interactions dominate the crystal structures of all of the solvates, while the Coulombic, polarization and repulsion terms play a lesser role. There are a few exceptions: for [**Fel+FA**] and [**Fel+N-MeFA**], the contribution of the Coulombic interaction is slightly larger compared to that for the rest of the solvates due to extra hydrogen bonds formed between **Fel** and the solvent molecules. It should be noted that the crystal lattice energies (E_{latt}) for all of the solvates are closely comparable and independent of the packing arrangements. The average magnitude of E_{latt} for all of the crystals is found to be 111.4 kJ·mol^{-1}, with a standard deviation of 5.2 kJ·mol^{-1} (4.7%).

Table 2 The results of PIXEL calculations: lattice energies (E_{latt}), Coulombic energies (E_{coul}), polarization energies (E_{pol}), dispersion energies (E_{disp}) and repulsion (E_{rep}) energies are in kJ·mol^{-1}

	E_{coul}	E_{pol}	E_{disp}	E_{rep}	E_{latt}
[**Fel+FA**]	-72.7	-27.2	-103.6	88.3	-115.1
[**Fel+N-MeFA**]	-62.4	-26.0	-109.4	81.5	-116.3
[**Fel+ATN**]	-48.2	-20.8	-123.1	88.7	-103.4
[**Fel+DMSO**]	-52.9	-29.8	-117.4	90.8	-109.4
[**Fel+DMF**]	-52.6	-24.3	-110.1	83.9	-103.1
[**Fel+DMAA**]	-56.7	-31.3	-128.5	108.5	-108.1
[**Fel+DMEU**]	-57.0	-27.7	-138.3	106.7	-116.3
[**Fel+APN**]	-52.1	-23.1	-135.3	95.0	-115.5
[**Fel+TMU**]	-53.0	-23.6	-123.9	84.9	-115.6

Although the total crystal lattice energies are similar, the energy distribution between different types of molecules in the solvates is distinguishable (Fig. 4). It is evident that for the crystals with a "back-to-back" arrangement, the **Fel-Fel** interactions provide the largest contribution to the lattice energy, while the solvates with a "side-on" organization are mainly stabilized by **Fel-Solv** interactions, with the **Fel-Fel** term being less prominent. This supports the assumption made above that the structures based on "side-on" interactions are expected to be less stable with respect to their **Fel-Fel** interactions. The transformation from the "back-to-back" to the "side-on" arrangement occurs at certain value of V_{vdw} for the solvent molecule, which is apparently large enough to stabilize the structure *via* more stabilizing **Fel-Solv** interactions. The overall similarity of the E_{latt} values indicates an effective distribution of all intermolecular interactions in the crystals so that the total lattice energies of the systems remain practically unchanged.

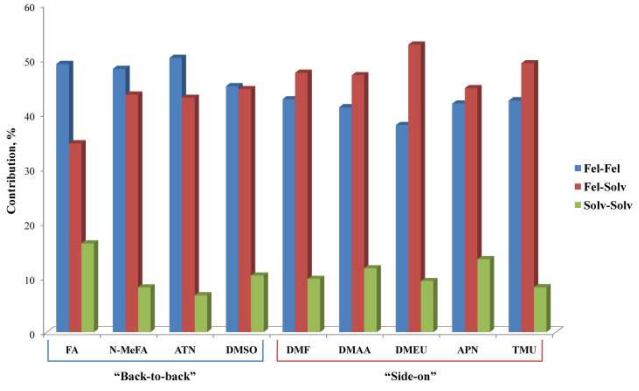

Fig.4 The relative contributions of the intermolecular interaction energies between the different types of molecules in the solvates calculated using the PIXEL method

As a next step, all of the solvate crystal structures were compared using the Crystal Packing Similarity module[19] implemented in Mercury,[20] in order to identify isostructural systems. For the "back-to-back" structures, the search did not reveal any similarity involving a statistically significant number of overlaid molecules (considered to be $n > 10$ and $rmsd_n < 1$). However, comparison of the crystal structures of [**Fel+DMF**] and [**Fel+DMAA**], which are "side-on" arranged, indicates that these two crystals contain the same principal substructure of the **Fel** molecules (n = 20, $rmsd_n$ = 0.350 Å). (see Fig. S5 in the Supporting Information). For the rest of the "side-on" structures the search did not show any further satisfactory match. Thus, only two solvates are found to be isostructural.

Thermal analysis

In the present study, DSC, TGA and HSM were used to assess the stability of the [**Fel+ATN**], [**Fel+APN**] and [**Fel+DMSO**] solvate crystals. Detailed thermal analyses of the pure felodipine polymorphs and a number of different solvates have been reported previously.[7, 12, 13] It has to be pointed out that the preparation and measurement procedures were unified for all the solvates in order to avoid the influence of those factors on the results of thermal analysis. The DSC curves are shown in Fig. 5, and the thermal data are tabulated in Table 3. For [**Fel+APN**] and [**Fel+DMSO**], DSC thermograms show only one endotherm which corresponds to the desolvation and melting processes. This thermal behaviour was found to be a common phenomenon for all of the felodipine solvates reported so far.[12, 13] By contrast, [**Fel+ATN**] shows a broad desolvation peak over the range ~70-

90°C, which is followed by melting of felodipine form I. The onset desolvation temperature is in good agreement with the data published by Rollinger and Burger.[10]

Table 3 shows clearly that boiling points of the solvents are considerably higher than the temperatures of desolvation of the corresponding solvates. For [**Fel**+**ATN**], however, the boiling point of the solvent, which is significantly lower than that for other solvents, is found to be *ca.* 13.8°C lower than the desolvation temperature. In the solvates with high-boiling point liquids, the solvent does not evaporate completely as it is released from the crystal, and it partly dissolves the desolvated felodipine, as seen in HSM experiments (Figure S6-S8 in the Supporting Information). It should be noted that the mentioned processes can affect the desolvation enthalpies derived from the DSC experiment, so direct comparison of those would not be quite correct.

Weight loss measurements in the TGA analysis are consistent with the DSC and HSM results (see Figure S9-S11 in the Supporting Information). The TGA curve for [**Fel**+**ATN**] indicates a classical one-step loss of solvent over the range ~70-90°C, while for [**Fel**+**APN**] and [**Fel**+**DMSO**], a continuous weight loss is observed over a temperature range 80–250°C. The TGA data for the latter solvates show several consecutive processes taking place during heating. The first step corresponds to loss of solvent and solvent evaporation (80-230°C), while further heating leads to **Fel** decomposition (above 230°C).

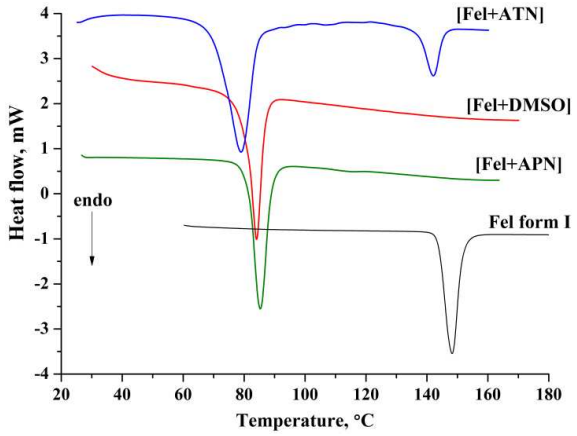

Fig.5 DSC curves of felodipine solvates and felodipine (form I) recorded at 10°C·min^{-1} heating rate

Table 3 Thermophysical data for the felodipine solvates

	T_{desolv}, °C (onset)	ΔH_{desolv}, kJ mol^{-1}	T_{boil}, °C
[Fel+ATN]	70.8 ± 0.4	46.0 ± 0.9	56.0
[Fel+APN]	81.5 ± 0.5	47.4 ± 0.7	202.0
[Fel+DMSO]	80.5 ± 0.5	41.4 ± 0.6	189.0
[Fel+DMAA][a]	110.6± 0.2	44.8 ± 0.5	165.1
[Fel+DMEU][a]	95.9 ± 0.2	34.4± 0.5	225.0
[Fel+TMU][a]	92.5 ± 0.2	31.0 ± 0.5	176.5
[Fel+FA][b]	122.7± 0.5	39.8 ± 0.9	210.0
[Fel+N-Me-FA][b]	84.8 ± 0.2	38.4 ± 0.4	182.6
[Fel+DMF][b]	82.1 ± 0.3	29.5 ± 0.3	153.0

[a] Data taken from ref.13;

[b] Data taken from ref.12

Despite the large difference in the solvent boiling points, the desolvation onset temperatures of the solvates are closely comparable. Most of the systems lie in a narrow temperature range between 80 and 100°C. The [**Fel**+**FA**] and [**Fel**+**DMAA**] solvates show the highest thermal stability, whereas [**Fel**+**ATN**] is found to be the least thermally stable.

It is evident that there is no correlation between the desolvation temperature of the solvates and the solvent boiling points. Usually thermal stability correlates with the boiling point of the solvent for solvates where the solvent molecules (guests) are weakly bound to the host molecules and situated in voids formed by the host structure.[21] The PIXEL calculations for the **Fel** solvates reveal that the contributions to the lattice energy from the **Fel-Fel** and **Fel-Solv** interactions are comparable (Fig. 4). The **Fel-Solv** interactions comprise 35-44% in the crystals with a "back-to-back" packing arrangement and 45-53% in the solvates with a "side-on" organization. The solvate thermal stability depends on various factors such as the packing arrangement of felodipine and solvent molecules, the solvent accommodation in the structures as well as the desolvation mechanism of the solvate. For example, the difference in onset temperature between the [**Fel**+**DMAA**] and [**Fel**+**DMF**] isostructural solvates equals *ca.* 28.5°C, which is considerably larger than the average value for the structurally unrelated crystals. Similar results have recently been observed for phenobarbital solvates.[22]

Solution calorimetry

In order to establish the thermodynamic characteristics for formation of the felodipine solvates, and to estimate their thermodynamic stability, solution calorimetry experiments were carried out for felodipine in the respective solvents. For [**Fel**+**ATN**], solution calorimetry was not performed due to low stability of the solvate at room temperature and high volatility of acetone as a solvent, which can easily affect the experimental results. The results are summarized in Table 4 (see Table S1 in the Supporting Information for the full data set).

Table 4 Solution enthalpies, $\Delta H°_{sol}$, and calculated enthalpies of formation, $\Delta H°_{f}$, at 298 K (kJ mol^{-1})

	$\Delta H°_{sol}$(Fel)$_{Solv}$	$\Delta H°_{sol}$([Fel+Solv])$_{Solv}$	$\Delta H°_{f}$([Fel+Solv])
[Fel+APN]	11.1 ± 0.2	27.1 ± 0.2	–16.0 ± 0.4
[Fel+DMSO]	15.2 ± 0.1	30.8 ± 0.3	–15.6 ± 0.4
[Fel+DMAA][a]	10.9 ± 0.2	29.8 ± 0.3	–18.8 ± 0.5
[Fel+DMEU][a]	7.3 ± 0.2	25.9 ± 0.3	–18.6 ± 0.5
[Fel+TMU][a]	4.1 ± 0.1	23.0 ± 0.3	–18.9 ± 0.4

[a] Data taken from ref.13.

For all of the solvates, the enthalpies of formation derived from the calorimetric data are similar, despite the difference in the crystal packing arrangements. It should be noted that enthalpy of formation is an integral parameter which indicates the difference between the crystal lattice energy of a solvate and pure **Fel**. Therefore, it can be deduced that the solvates should have comparable E_{latt} values, which is consistent with the PIXEL calculations.

Analysis of Hirshfeld Surfaces

Analysis of Hirshfeld surfaces is found to be a useful tool for description of various types of intermolecular contacts in molecular crystals.[23] The method has been widely used for polymorphs,[24] solvates[25] and co-crystals of APIs.[26] The relative contributions of the important intermolecular contacts of **Fel** in

the solvates are compared to those of felodipine (Form I) in Fig.6. (The 2-D fingerprint plots for the solvates are shown in Fig. S12 in the Supporting Information).

For all of the solvates, the H···H contacts comprise approximately half of the total Hirshfeld surfaces (50.5 % in average), which indicates that the crystal structures are mainly stabilized by van der Waals interactions. A substantial part of each Hirshfeld surface is occupied by the C…H, O…H and Cl…H contacts. Their relative contributions to the Hirshfeld surfaces are comparable, comprising on average 14.9% for C…H, 16.0% for O…H and 14.4% for Cl…H. The O…H contacts are the shortest ones in all of the solvates. It was noted that a ratio of the relative contributions of the main intermolecular contacts in the solvates remains practically unchanged: H…H/C…H/O…H/Cl…H ≈ 1/0.3/0.3/0.3. It might be reasonable to assume that this ratio indicates the most efficient crystal packing.

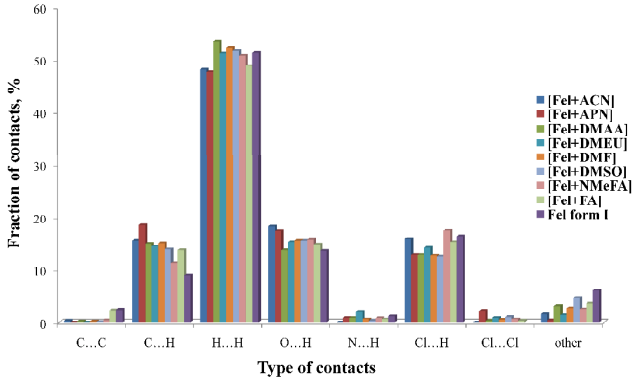

Fig.6 The relative contribution of the intermolecular contacts to the Hirshfeld surface area for **Fel** in the solvates

For pure felodipine form I, the contribution of the H···H contacts remains at the same level, comprising essentially half of the total surface. The O…H and Cl…H contacts also demonstrate similar contributions. A significant difference is observed for the C···H interactions, whose contribution is lower by approximately 40% in **Fel** compared to the average value in the solvates.

Aqueous dissolution

Dissolution profiles for [**Fel**+**APN**], [**Fel**+**DMSO**], the previously reported felodipine solvates and felodipine (form I) are shown in Fig. 7. For [**Fel**+**ATN**], the dissolution experiment was not performed due to its low stability at room temperature. It is seen that all of the dissolution profiles have a similar shape. In terms of the "spring and parachute" concept[27] the dissolution profiles for the felodipine solvates show clearly a "spring" phase, while the "parachute" effect is observed only for a short time. During the first hour of dissolution, the concentration of felodipine is increased by several times compared to the form I of API. This is followed by fast crystallization of felodipine, and the latter process lasts from 1 to 6 hours depending on the solvate stability. The experiment shows that the least stable solvate is [**Fel**+**DMSO**], while the longest life-time is observed for [**Fel**+**APN**] and [**Fel**+**TMU**].

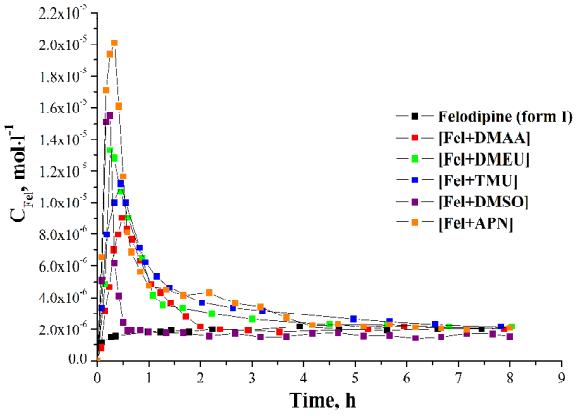

Fig.7 Dissolution profiles of the felodipine solvates and felodipine (form I) in water at 25.0 °C.

Conclusions

Three new solvates of felodipine with structurally related common organic solvents, acetone, dimethyl sulfoxide and acetophenone, have been obtained and their crystal structures determined. All of the currently established solvate crystal structures can be conventionally divided into two groups with respect to the felodipine packing arrangement: structures based on "back-to-back" interactions between felodipine molecules and crystals where the molecules are arranged in a "side-on" manner. The felodipine packing arrangement is found to depend on the van der Waals volume (V_{vdw}) of the solvent molecule. At relatively small V_{vdw} (40 Å^3 < V_{vdw} < 70 Å^3) the felodipine molecules tend to form a "back-to-back" structure, while formation of the "side-on" structure is observed for V_{vdw} > 70 Å^3. PIXEL calculations reveal that in the crystals with a "back-to-back" arrangement, the **Fel-Fel** interactions provide the largest contribution to the lattice energy, while the solvates with a "side-on" organization are mainly stabilized by **Fel-Solv** interactions, with the **Fel-Fel** contribution being less prominent. DSC studies show that the desolvation onset temperatures of the solvates are closely comparable, despite quite large differences in the solvent boiling points. For most of the systems, the desolvation occurs in a narrow temperature range between 80 and 100°C. The enthalpies of formation derived from the calorimetric data for the solvates are found to be similar, despite the difference in V_{vdw} of the solvent molecules. Analysis of Hirshfeld surfaces indicates that there is no significant difference in the distribution of the main intermolecular contacts between the solvates, and the following ratio is suggested: H…H/C…H/O…H/Cl…H ≈ 1/0.3/0.3/0.3. The aqueous dissolution profiles for all solvates demonstrate only a clear "spring" phase, while the "parachute" effect is observed over a time period from 1 to 6 hours depending on the solvate stability.

Acknowledgements

This work was supported by a grant from the President of the Russian Federation no. МК- 67.2014.3 and Russian Foundation for Basic Research (project № 14-03-31001). We thank "the

upper Volga region centre of physicochemical research" for technical assistance with DSC and TG experiments.

Notes and references

[a]*Institution of Russian Academy of Sciences, G.A. Krestov Institute of Solution Chemistry RAS, 153045 Ivanovo, Russia. Fax: +7 4932 336237; Tel: +7 4932 533784; E-mail: glp@isc-ras.ru.*
[b]*Department of Physics, Chemistry and Pharmacy, University of Southern Denmark, Campusvej 55, 5230 Odense M, Denmark.*
[§]*Current address: University of Cambridge, Department of Chemistry, Lensfield Road, CB2 1EW, United Kingdom.*

† Electronic Supplementary Information (ESI) available: the results of the Crystal Packing Similarity analysis for the [**Fel**+**DMAA**] and [**Fel**+**DMF**] solvates, HSM pictures and TGA traces, 2D fingerprint plots of the felodipine solvates, the full data set of the solution calorimetry experiments. See DOI: 10.1039/b000000x/

1. Bernstein, J. *Polymorphism in Molecular Crystals*; Clarendon Press: Oxford, U.K., 2002.
2. S. Byrn, R. Pfeiffer, M. Ganey, C. Hoiberg and G. Poochikian, *Pharm. Res.*, 1995, **12**, 945.
3. U. J. Griesser, *The Importance of Solvates.* In *Polymorphism in the Pharmaceutical Industry*; Hilfiker, R., Eds.; Wiley-VCH: Weinheim, 2006.
4. P. W. Cains. *Classical Methods of Preparation of Polymorphs and Alternative Solid Forms.* In *Polymorphism in Pharmaceutical Solids*, *Second Edition*; Brittain, H.G., Eds.; Informa Healthcare: New York, 2009.
5. a) P.A. Todd and D. Faulds. Felodipine: a review of the pharmacology and therapeutic uses of the extended release formulation in cardiovascular disorders, Drugs 44 (1992) 251; b) N. Nussinovitch, J. Carroll, A. Shamiss, E. Grossman, A. Katz, C. Rachima and T. Rosenthal, *J. Hum. Hypertens.*, 1996, **10**, S165.
6. a) R. Fossheim, *J. Med. Chem.*, 1986, **29**, 305; b) J. Kerč, S. Srčič, U. Urleb, I. Zupančič, G. Lahajnar, B. Kofler and J. Smid-Korbar, *Int. J. Pharm.*, 1992, **87**, 1.
7. A. O. Surov, K. A. Solanko, A. D. Bond, G. L. Perlovich and A. Bauer-Brandl, *Cryst. Growth Des.*, 2012, **12**, 4022.
8. A. O. Surov, K. A. Solanko, A. D. Bond, A. Bauer-Brandl and G. L. Perlovich, *CrystEngComm*, 2014, **16**, 6603.
9. K. A. Solanko, A. O. Surov, G. L. Perlovich, A. Bauer-Brandl and A. D. Bond, *Acta Cryst.*, 2012, **C68**, o456.
10. J. M. Rollinger and A. Burger, *J. Pharm. Sci.*, 2001, **90**, 949.
11. B. Lou, D. Boström and S. P. Velaga, *Cryst. Growth Des.*, 2009, **9**, 1254.
12. G. L. Perlovich, S. V. Blokhina, N. G. Manin, T. V. Volkova and V. V. Tkachev, *CrystEngComm*, 2012, **14**, 8577.
13. A. O. Surov, K. A. Solanko, A. D. Bond, A. Bauer-Brandl and G. L. Perlovich, *CrystEngComm*, 2013, **15**, 6054.
14. N. G. Manin, A. Fini and G. L. Perlovich, *J. Therm. Anal. Calorim.* 2011, **104**, 279.
15. J. D. Cox and G. Pilcher, *Thermochemistry of Organic and Organometallic Compounds*, Academic Press, London, 1970; p 643.
16. a) A. Gavezzotti, *J. Phys.Chem.*, 2003, **B107**, 2344; b) A. Gavezzotti, *Mol. Phys.*, 2008, **106**, 1473.
17. A. J. Cruz-Cabeza, G. M. Day and W. Jones, *Phys. Chem. Chem. Phys.,* 2011, **13**, 12808.
18. a) A. Gavezzotti, *Z. Kristallogr.*, 2005, **220**, 499. b) A. Gavezzotti, *New J. Chem.*, 2011, **35**, 1360. c) L. Maschio, B. Civalleri, P. Ugliengo and A. Gavezzotti, *J. Phys. Chem. A.*, 2011, **115**, 11179.
19. J. A: Chisholm and S. Motherwell, *J. Appl. Crystallogr.* 2005, **38**, 228.
20. C. F. Macrae, P. R. Edgington, P. McCabe, E. Pidcock, G. P. Shields, R. Taylor, M. Towler and J. van de Streek, *J. Appl. Crystallogr.* 2006, **39**, 453.
21. a) L. R. Nassimbeni, *Acc. Chem. Res.*, 2003, **36**, 631; b) S. Aitipamula, P. S. Chow, and R. B. H. Tan, *J. Mol. Struct.*, 2011, **1005**, 134; c) A. Bērziņš, T. Rekis and A. Actiņš, *Cryst. Growth Des.*, 2014, **14**, 3639.
22. N. Zencirci, U. J. Griesser, T. Gelbrich, V. Kahlenberg, R. K. R. Jetti, D. C. Apperley and R. K. Harris, *J. Phys. Chem. B*, 2014, **118**, 3267.
23. a) M. A. Spackman and D. Jayatilaka, *CrystEngComm*, 2009, **11**, 19; b) M.A. Spackman and J. J. McKinnon, *CrystEngComm*, 2002, **4**, 378.
24. a) L. Vella-Zarb, R. E. Dinnebier and U. Baisch, *Cryst. Growth Des.* 2013, **13**, 4402; b) A. J. Rybarczyk-Pirek, L. Chęcińska, M. Małecka and S. Wojtulewski, *Cryst. Growth Des.* 2013, **13**, 3913; c) J. B. Nanubolu, B. Sridhar, V. S. P. Babu, B. Jagadeesh and K. Ravikumar, *CrystEngComm*, 2012, **14**, 4677; d) A. A. Hoser, K. N. Jarzembska, Ł. Dobrzycki, M. J. Gutmann and K. Woźniak, *Cryst. Growth Des.*, 2012, **12**, 3526; e) K. Durka, A. A. Hoser, R. Kamiński, S. Luliński, J. Serwatowski, W. Koźmiński and K. Woźniak, *Cryst. Growth Des.*, 2011, **11**, 1835; f) R. D. L. Johnstone, A. R. Lennie, S. F. Parker, S. Parsons, E. Pidcock, P. R. Richardson, J. E. Warren and P. A. Wood, *CrystEngComm*, 2010, **12**, 1065; g) J. J. McKinnon, F. P. A. Fabbiani and M. A. Spackman, *Cryst. Growth Des.*, 2007, **7**, 755.
25. a) D. M. Kamiński, A. A. Hoser, M. Gagoś, A. Matwijczuk, M.Arczewska, A. Niewiadomy and K. Woźniak, *Cryst. Growth Des.* 2010, **10**, 3480; b) F. P. A. Fabbiani, L. T. Byrne, J. J. McKinnon and M. A. Spackman, *CrystEngComm*, 2007, **9**, 728.
26. a) G. Bolla, S. Mittapalli and A. Nangia, *CrystEngComm*, 2014, **16**, 24; b) Y.-H. Luo and B.-W. Sun, *Cryst. Growth Des.*, 2013, **13**, 2098; b) Y.-H. Luo, C.-G. Zhang, B. Xu and B.-W. Sun, *CrystEngComm*, 2012, **14**, 6860; c) H. F. Clausen, M. S. Chevallier, M. A. Spackman and B. B. Iversen, *New J. Chem.*, 2010, **34**, 193.
27. a) H. R. Guzmán, M. Tawa, Z. Zhang, P. Ratanabanangkoon, P. Shaw, C. R. Gardner, H. Chen, J.-P. Moreau, Ö. Almarsson and J. F. Remenar, *J. Pharm. Sci.*, 2007, **96**, 2686; b) N. Schultheiss and A. Newman, *Cryst. Growth Des*. 2009, **9**, 2950; c) J. Chen, B. Sarma, J. M. B. Evans and A. S. Myerson, *Cryst Growth Des.* 2011, **11**, 887; d) R. Thakuria, A. Delori, W. Jones, M. P. Lipert, L. Roy and N. Rodríguez-Hornedo, *Int. J. Pharmaceut.,* 2013, **453**, 101; e) N. J. Babu and A. Nangia, *Cryst. Growth Des.* 2011, **11**, 2662.

Diversity of felodipine solvates: structure and physicochemical properties

Artem O. Surov,[a] Katarzyna A. Solanko,[b] Andrew D. Bond,[b§] Annette Bauer-Brandl[b] and German L. Perlovich[*a]

[a] G.A. Krestov Institute of Solution Chemistry, Russian Academy of Sciences, Ivanovo, Russia; [b]Department of Physics, Chemistry and Pharmacy, University of Southern Denmark, Odense, Denmark.
[§] Current address: University of Cambridge, Department of Chemistry, Lensfield Road, CB2 1EW, United Kingdom.

Solvates of the calcium-channel blocking agent felodipine with three structurally related common organic solvents, acetone (**ATN**), dimethyl sulfoxide (**DMSO**) and acetophenone (**APN**), are described. A relationship between the felodipine packing arrangement in all known solvates and the van der Waals volume of the solvent molecule is established. The solvates were investigated by a wide spectrum of experimental methods and approaches: X-ray diffraction, DSC, TG, HSM and solution calorimetry. Intermolecular interaction energies in the crystals are examined using the PIXEL approach in order to rationalize the difference between alternative molecule packing arrangements.

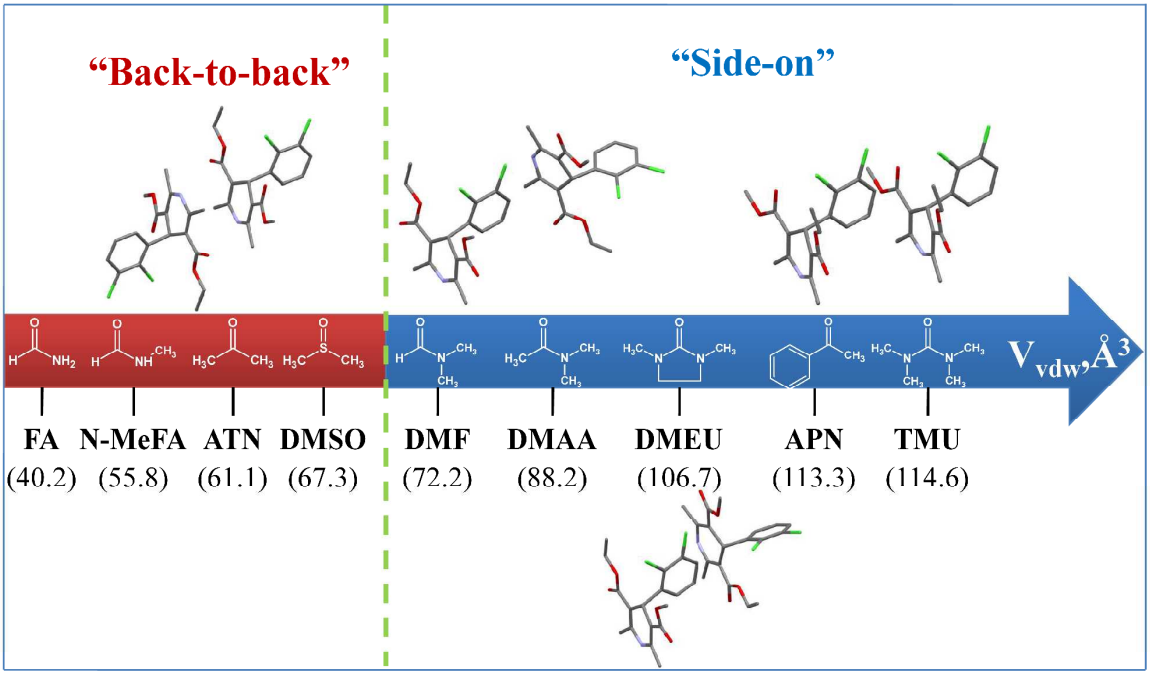

* To whom correspondence should be addressed:
Tel.: (+7) 4932 533784; fax: (+7) 4932 336237; E-mail address: glp@isc-ras.ru